Received: January 6, 2020

INASS

International Journal of
Intelligent Engineering & Systems

http://www.inass.org/

Odor Source Searching in Mechanical Turbulent Airflow Using a Mobile Robot

Helmy Widyantara[1,2] **Muhammad Rivai**[1]* **Totok Mujiono**[1]

[1] *Department of Electrical Engineering, Institut Teknologi Sepuluh Nopember, Surabaya, Indonesia*
[2] *Institut Teknologi Telkom Surabaya, Indonesia*
* Corresponding author's Email: muhammad_rivai@ee.its.ac.id

Abstract: Localization of gas leak sources is needed especially in industrial areas and the environments. Because some gases are dangerous to humans, the use of robots equipped with gas sensors is often employed to find the odor or gas sources. Rapid finding of the target is the main key to minimize the potential danger caused by several toxic, flammable and explosive gas compounds. This paper discusses the searching for odor source in an obstacle environment using a mobile robot, in which the presence of the obstacle can produce mechanical turbulent airflow. The turbulent airflow causes odor plume to change the direction of its spread, making it difficult for the mobile robot to find the location of the odor source. The mobile robot used in this study is equipped with a new method of combining gas sensors and wind sensors to find the odor source. The experimental results show that the combination of the two types of sensors can increase the success rate of 90% and 70% in laminar, and mechanical turbulent airflow, respectively, compared to the use of gas sensors only. In addition, this combination of sensors can improve the performance of the mobile robot including shorter travel distance and travel time by 2.4% and 45.9%, respectively.

Keywords: Mechanical turbulent airflow, Mobile robot, Odor source searching.

1. Introduction

Tracking the location of gas leaks carried out by humans has a high risk [1]. For tasks that endanger human safety, the use of mobile robots is an appropriate solution [2, 3]. The use of electronic nose integrated in the mobile robot allows to assist the process of tracking the location of the gas source [4-6], such as for robot navigation [7] and localization of odor sources in the room [8].

There are several odor plume search algorithms namely surge-spiral, upwind and zig-zag. The zig-zag method is more efficient when the robot moves faster than odor plume or airflow, while the upwind method is better when the robot moves slower than odor plume [9]. These methods have difficulty in finding target when there is a change in wind direction. This results in a change in the direction of the odor plume which causes the robot to lose the track and it will take a long time to find the odor source.

The use of wind direction sensors could improve the performance of tracking the odor plume. The wind sensors can help robots to re-find traces of odor plume which lost due to changes in wind direction [10, 11]. In real conditions, there are several obstacles in the search area of gas leaks. The presence of the obstacle certainly causes mechanical turbulence in the airflow, in which the turbulence occurs because the airflow crashes into the obstacle [12]. Tracking odor plume in areas where turbulence does not occur can be seen in Fig. 1(a). In this case, the gas is spread in an advection and diffusion without accompanied by turbulence of airflow [13] [14]. In contrast with the laminar airflow, gas is not only spread by advection and diffusion but also distributed randomly due to turbulence of airflow [15] shown in Fig. 1 (b).

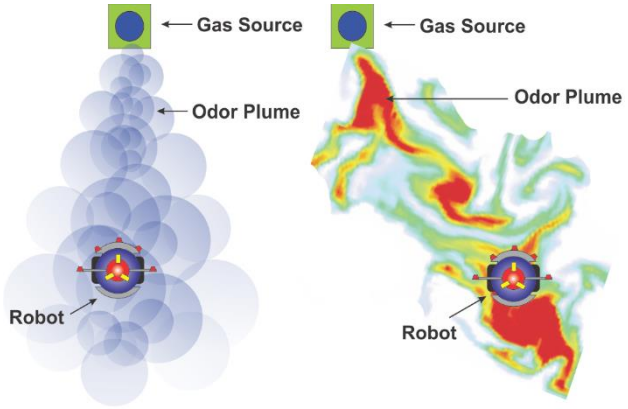

(a) (b)

Figure. 1 Odor plume searching on conditions: (a) laminar and (b) turbulent airflow

Turbulence can increase the level of difficulty in finding the location of a gas leak; thus, it requires a robust odor plume tracking method. The aim of this work is to develop a new method of odor searching by a mobile robot using a combination of gas sensors and wind sensors. This combination of the sensors is expected to solve the problems of tracking odor plume in areas with obstacles and dynamic wind conditions. A more detailed discussion in this paper will be organized as follows. Research methods include the differential steering robot design, the odor plume tracking and the obstacle avoidance algorithms, as well as the gas sensor and wind sensor designs. In the result and analysis will discuss the experimental setup, the experimental results of the stereo gas sensor and the wind direction sensor, as well as the results of experiments on the mobile robot in searching for odor source in laminar and turbulent airflows. This section also discusses the comparison of performance between the mobile robot equipped with gas sensors only and when the mobile robot equipped with a combination of gas sensors and wind sensors.

2. Research method

A method which is often used to find the location of an odor source usually consists of three stages including searching for odor plume, trace the odor plume, and gas source declaration. A navigation system that combines wind direction sensors and gas sensors could increase the success rate of finding gas leak locations [16]. The robot is expected to find the location of the gas leak even though it must pass the obstacle that can cause turbulence in airflow. Therefore, an odor plume tracking method is needed in dynamic wind conditions.

2.1 Differential steering robot

In this study, we use a robot with a differential steering system type which is relatively more flexible in maneuvering. This robot design is shown in Fig. 2. The robot is equipped with gas sensors. wind sensors, and obstacle sensors. The gas sensors used in this study are metal oxide type. Experiments about wind direction sensors has been discussed in our previous article [10]. The obstacle sensor consists of three ultrasound proximity sensors.

The differential steering system can be seen in Fig. 3. For the length of the wheel radius r, and the rotation speed of the right ω_R and left wheels ω_L, then the linear velocity of the right and left wheels can be found by the following equation:

$$v_R(t) = r\omega_R(t) \quad (1)$$

$$v_L(t) = r\omega_L(t) \quad (2)$$

When the robot makes a momentary spinning motion with the length of the radius R measured from the center of rotation and the center of the two wheels, the rotation speed can be calculated as:

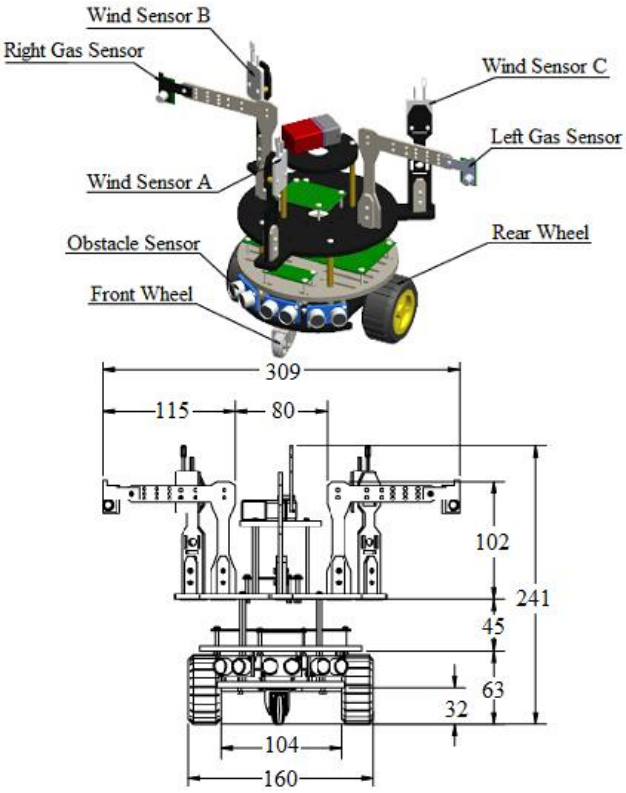

Figure. 2 The Platform and dimension of the mobile robot

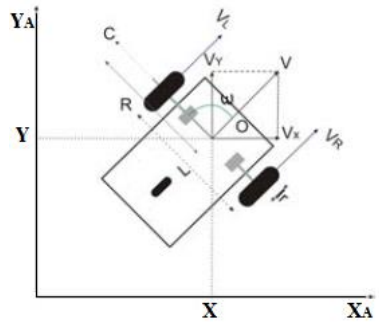

Figure. 3 Differential steering system

$$\omega(t) = \frac{v_R}{R+\frac{L}{2}} \tag{3}$$

$$\omega(t) = \frac{v_L}{R-\frac{L}{2}} \tag{4}$$

The linear velocity of robot $v(t)$ and the rotational speed of robot $\omega(t)$ can be determined based on both the linear velocity of the wheel. The matrix can be presented as follows:

$$\begin{bmatrix} v(t) \\ \omega(t) \end{bmatrix} = \begin{bmatrix} \frac{1}{2} & \frac{1}{2} \\ \frac{1}{L} & -\frac{1}{L} \end{bmatrix} \begin{bmatrix} v_R(t) \\ v_L(t) \end{bmatrix} \tag{5}$$

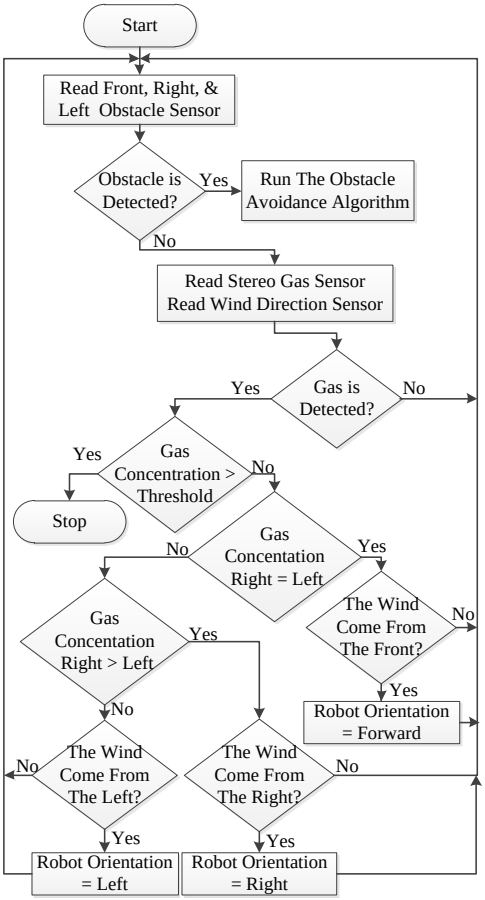

Figure. 4 The odor plume tracking algorithm

Eq. (5) shows the direct kinematics relation between the linear velocity of the robot wheels to the linear and angular speed of the robot, while Eq. (6) shows the opposite relation.

$$\begin{bmatrix} v_R(t) \\ v_L(t) \end{bmatrix} = \begin{bmatrix} 1 & \frac{L}{2} \\ 1 & -\frac{L}{2} \end{bmatrix} \begin{bmatrix} v(t) \\ \omega(t) \end{bmatrix} \tag{6}$$

2.2 Odor plume tracking

Odor plume tracking is carried out by utilizing a combination of stereo gas sensors and wind sensors. The odor plume searching algorithm is depicted as in Fig 4. The first step taken by the robot is to detect obstacle. If there is an obstacle, the robot will run the avoidance algorithm until it is free from the obstacle. Gas detection is carried out by stereo gas sensors mounted on the right and left of the robot. When gas is detected by the robot, an odor plume tracking is then performed using a combination of gas sensors and wind sensors.

2.3 Obstacle avoidance

The robot movement to avoid obstacle is highly dependent on the proximity sensors [17]. The robot will turn if one of the three ultrasonic sensors has a threshold value (d_T) below 30 cm. In this study, the three ultrasonic sensors are in the front (d_f), -45° on the left (d_l), and +45° on the right (d_r), as seen in Fig. 5 (a).

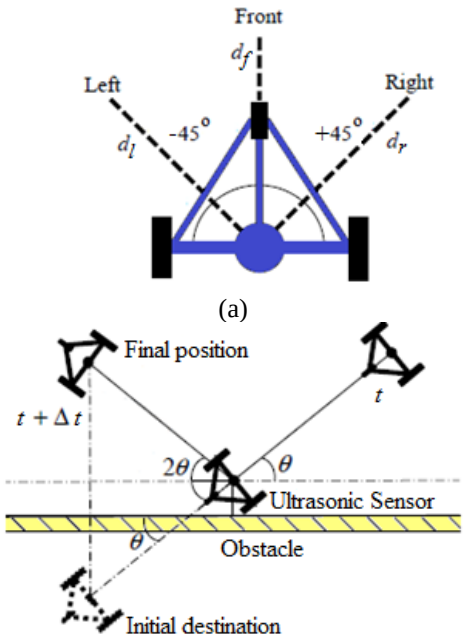

Figure. 5 Obstacle avoidance: (a) the sensor positions and (b) illustration when avoiding an obstacle

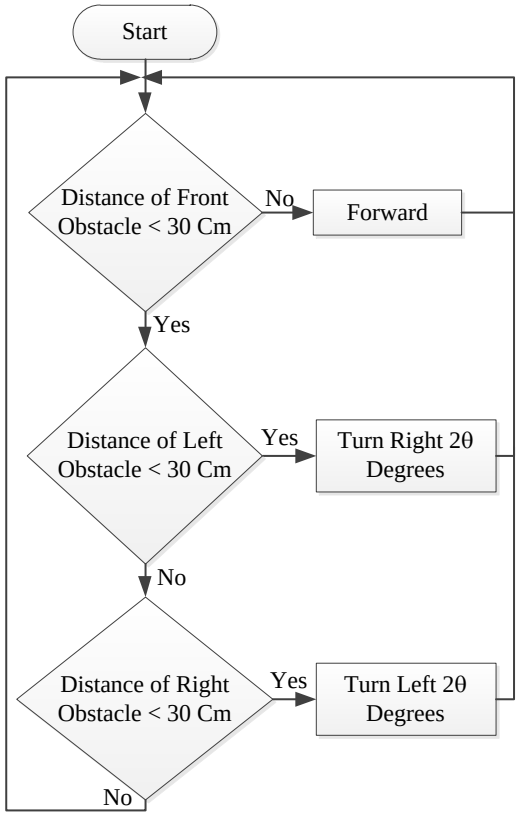

Figure. 6 Flowchart of the obstacle avoidance

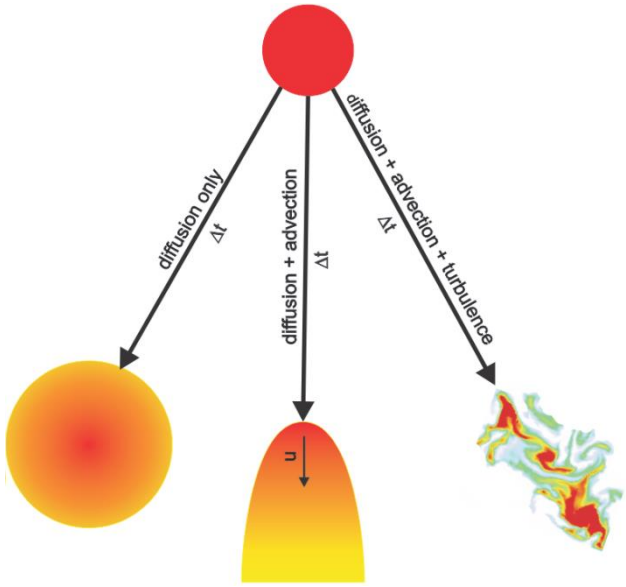

Figure. 7 The transports of a substance

Illustration of robot movement when detecting an obstacle can be seen in Fig. 5 (b). The turning angle 2θ of the robot can be calculated using the cosine function. When d_f and d_l are less than d_T, the robot will turn right at an angle expressed as:

$$\theta = arccos\left(\frac{2d_f - \sqrt{2d_l}}{2\sqrt{d_f^2 + d_l^2 - \sqrt{2}d_f d_l}}\right) \quad (7)$$

When d_f and d_r are less than d_T, the robot will turn left at an angle expressed as:

$$\theta = arccos\left(\frac{2d_f - \sqrt{2d_r}}{2\sqrt{d_f^2 + d_r^2 - \sqrt{2}d_f d_r}}\right) \quad (8)$$

The obstacle avoidance algorithm used in the robot is shown in Fig. 6. When there is no obstacle in the front, the robot will move forward. If the front and left distances to the obstacle are less than 30 cm, the robot will turn right at an angle of 2θ. Similarly, the action to turn to the left.

2.4 Advection and diffusion

Gas spreading can occur by advection alone, or a combination of advection and diffusion as shown in Fig. 7. Advection cause a formation of odor plume. In normal conditions, the odor plume will be distributed according to the direction of the wind flow. Turbulence in the airflow causes the spread of odor plume to be random. Turbulence of the airflow in the searching area for odor source can be caused by the presence of material around the location. Turbulence occurs because the airflow hits solid material, so the direction of movement becomes erratic.

Initially, turbulent airflow in this study was simulated with computational fluid dynamic (CFD) according to the actual test plant with a length of 200 cm and width of 180 cm. Meanwhile, the tube-shaped obstacle has a diameter of 10 cm and a height of 30 cm.

2.5 Gas sensor

There are several types of gas sensors with their advantages and disadvantages, based on the physico-chemical principles and sensitivity. They are divided into six groups, namely: metal oxide semiconductor (MOS), electro-chemical cell (EC), conducting polymer (CP), quartz crystal microbalance (QMB), surface acoustic wave (SAW), and photo ionization detector (PID) [18]. This study involved MOS type gas sensors, because it has a fast response and recovery time and is also sensitive to some gases at the ppm level [19]. MOS sensors work based on chemical reactions, the value of the sensor resistance depends on the concentration of gas in contact with the surface. The greater the gas concentration, the smaller the sensor resistance value.

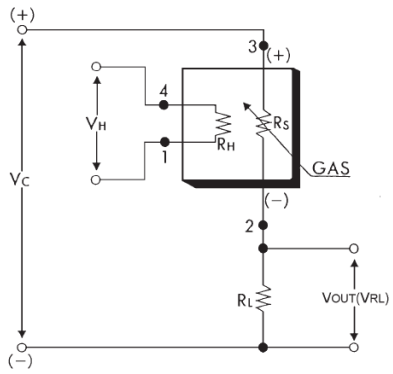

Figure. 8 TGS2611 gas sensor's wiring diagram

The relationship between sensor resistance and gas concentration can be seen in eq. (9), where R is the resistance of the metal-oxide sensor, C is gas concentration, A is gas response coefficient, and α is sensitivity. A wiring diagram on the TGS2611 series can be seen in Fig. 8.

$$R = A\,[C]^{-\alpha} \tag{9}$$

The value of Rs can be found by eq. (10).

$$Rs = \frac{V_C - V_{RL}}{V_{RL}}\,R_L \tag{10}$$

2.6 Wind sensors

The wind direction sensor in this study employs the thermal anemometer of the Rev. P Wind Sensor developed by Modern Devices using the positive temperature coefficient thermistors. A wire heated by an electric current will have thermal equilibrium with the environment. Electric power supply is proportional to the power lost due to convective heat transfer expressed as:

$$I^2 R_W = h.A_W(T_W - T_F) \tag{11}$$

$$R_W = R_R[1 + \alpha(T_W - T_R)] \tag{12}$$

where I is the input electric current, R_W is the wire resistance, T_W is the wire temperature, T_F is the fluid temperature, A_W is the projected wire surface area, h is the wire heat transfer coefficient, R_R is the resistance at the reference temperature T_R, and α is the thermal coefficient of resistance. In this type of anemometer, the faster the air flow, the greater the cooling effect [9].

3. Result and analysis

The odor source in this experiment uses gasoline vapor blown by an electric fan with an average speed of 2 mph. The obstacle is located at 70 cm in front of the odor source. The experimental setup carried out in this study is shown in Fig. 9.

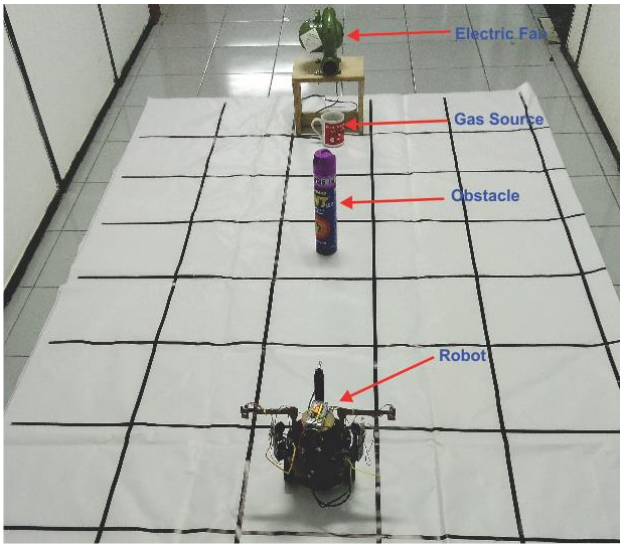

Figure. 9 The experimental setup

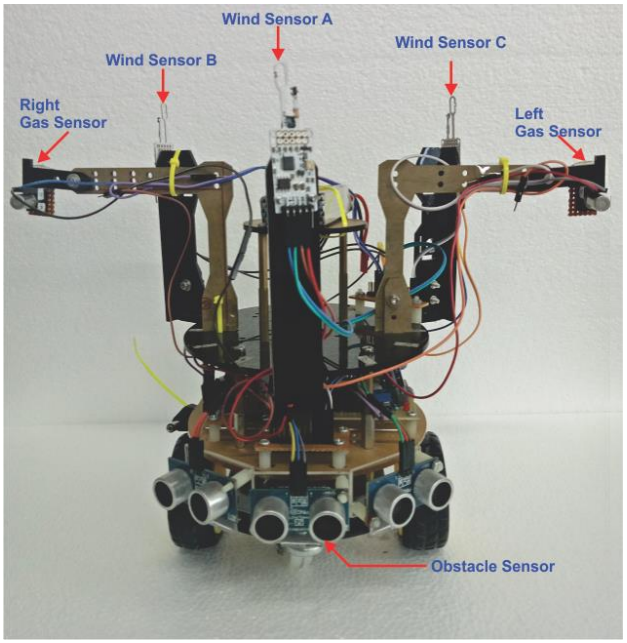

Figure. 10 The mobile robot used in the experiments

3.1 The olfactory mobile robot

The differential steering mobile robot design was constructed with acrylic material. The robot is equipped with 2 gas sensors, 3 wind sensors, and 3 proximity sensors. The robot dimensions have a width of 309 mm, height of 241 mm, and wheel diameter of 63 mm. This robot is supplied with a dc source of 9 volts which can move with linear speeds of between 471 and 2500 cm/s. The robot platform can be seen in Fig. 10.

3.2 Air flow generator

To illustrate the airflow patterns at the actual test plant, a simulation is performed first using CFD analysis on the SimFlow software. Fig. 11 illustrates laminar airflow in a plant without obstacles at 0.25, 0.5, and 0.75 seconds. Meanwhile, the turbulent airflow due to an obstacle is shown in Fig. 12.

3.3 Stereo gas sensor

The stereo gas sensor consists of two TGS 2611 gas sensors located at the top left and right of the robot. The sensor's analog signal is converted by an internal 10-bit analog-to-digital converter (ADC) embedded in the Arduino/Genuino 101 microcontroller. This experimental setup is illustrated in Fig. 13. In the initial position, the robot is located in several different positions (a, b, and c). The response of the stereo gas sensor is shown in Fig. 14. In position (b), it appears that the two sensors have a similar response. Meanwhile in position (a), the right sensor has a higher response than the left one which is the opposite of the sensor's response at position (c).

3.4 Wind direction sensor

In this study, the wind direction sensor is determined by the response of the three wind sensors. The normalized response of the sensors is shown in Fig. 15. The three sensors produce different patterns when subjected to several wind directions.

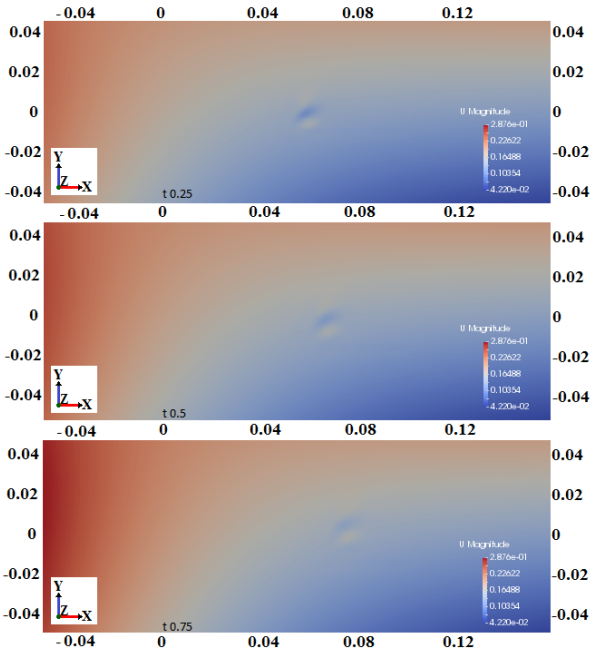

Figure. 11 Simulated airflow in a room without obstacles at different times

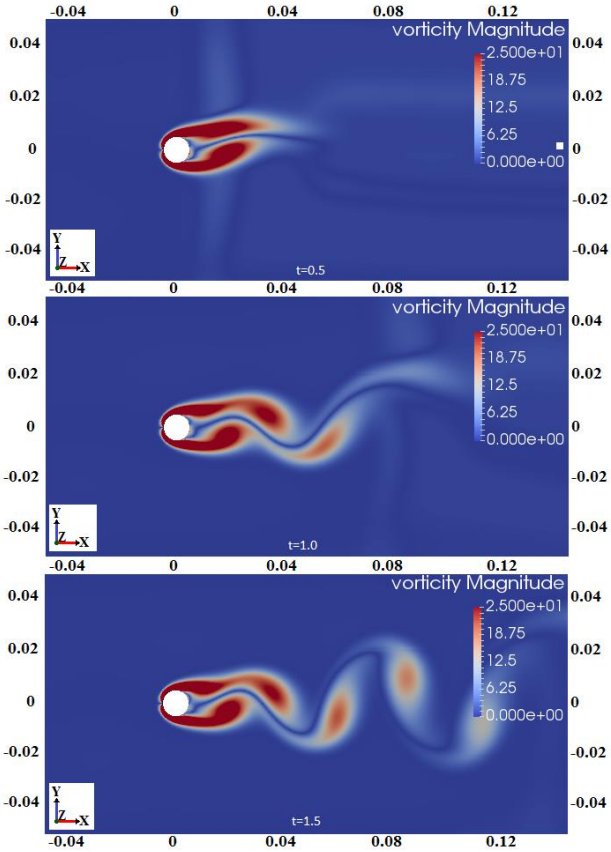

Figure. 12 Simulated airflow when crashing into an obstacle at different times

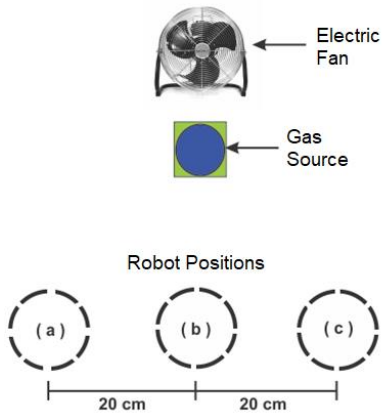

Figure. 13 Measurement of gas sensor response with several positions

3.5 Searching for odor source in laminar airflow

This experiment is regarding with the search for odor source as far as 100 cm by the mobile robot equipped with gas sensors without any obstacles. The success rate for finding odor sources is 50% as shown in Table 1. Meanwhile, the travel distance and travel time to find the odor source is shown in Table 2.

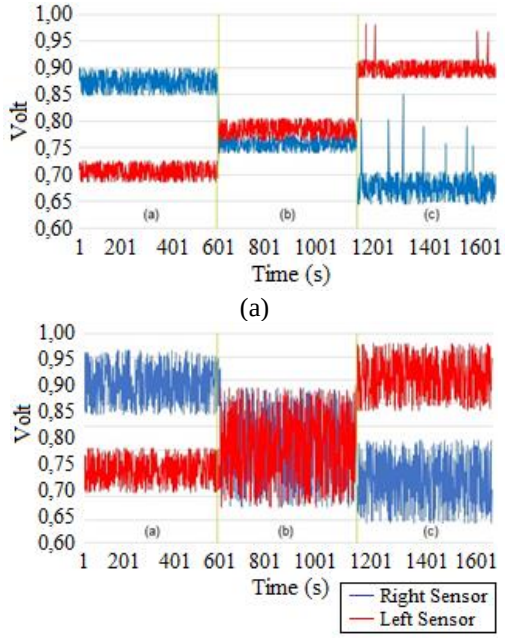

(a)

(b)

Figure. 14 The response from the stereo gas sensor with several positions of: (a) 50 cm and (b) 125 cm

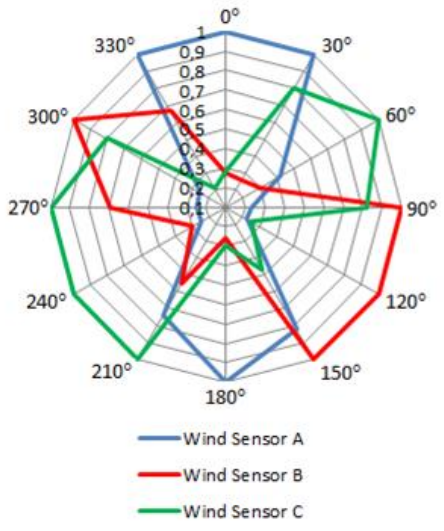

Figure. 15 Wind direction sensor

The next experiment is the search for wind source as far as 100 cm by the mobile robot equipped with wind sensors without any obstacles. The success rate for finding wind source is 100%. The travel distance and travel time to find the wind source is shown in Table 3. The robot's trajectory when tracking odor plume and wind source in laminar airflow is depicted in Fig. 16.

The next experiment aims to determine the ability of the mobile robot in tracking the odor source in the laminar airflow using a combination of gas sensors and wind sensors. The performance of the robot is shown in Table 4. The success rate for finding odor source is 90%.

Table 1. The success rate of the mobile robot equipped with gas sensors to find the odor source in laminar airflow

No	Success rate	
	Success	Failure
1	1	0
2	0	1
3	1	0
4	0	1
5	0	1
6	1	0
7	0	1
8	1	0
9	1	0
10	0	1

Table 2. The performance of the mobile robot equipped with gas sensors to find the odor source in laminar airflow

No	Travel Distance (cm)	Travel Time (seconds)
1	120	8
2	115	7
3	120	6
4	130	9
5	115	6
Average	**120**	**7.2**

Table 3. The performance the mobile robot equipped with wind sensors to find the wind source in laminar airflow

No	Travel Distance (cm)	Travel Time (seconds)
1	100	5
2	100	5
3	120	6
4	100	5
5	100	5
6	120	6
7	100	5
8	100	5
9	120	6
10	100	5
Average	**106**	**5.3**

3.6 Searching for odor source in mechanical turbulent airflow

This experiment aims to determine the ability of the mobile robot in tracking the odor source as far as

200 cm in the turbulent airflow. The performance of the robot in the search for odor source in mechanical turbulent airflow that use only gas sensors and a combination of gas sensors and wind sensors are shown in Tables 5 and 6, respectively. This shows that the mobile robot equipped with a combination of gas sensors and wind sensors is able to find odor source with shorter travel distance and travel time, which improve by 2.4%, and 45.9%, respectively. This method also has a higher success rate of 70%. The robot's trajectory when tracking odor plume in mechanical turbulent airflow is depicted in Fig. 17 and Fig. 18.

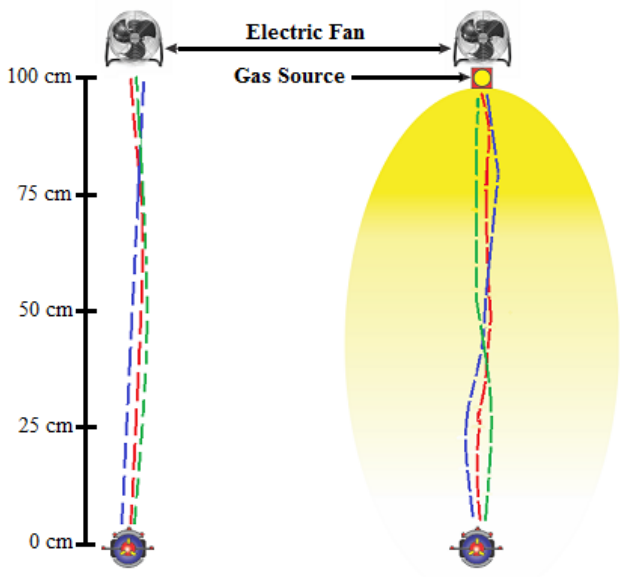

(a) (b)

Figure. 16 The robot's trajectory in laminar airflow when tracking: (a) odor plume and (b) wind source

Table 4. The performance of the mobile robot equipped with a combination of gas sensors and wind sensors to find the odor source in laminar airflow

No	Travel Distance (cm)	Travel Time (seconds)
1	120	6
2	100	5
3	120	6
4	120	6
5	120	6
6	100	5
7	100	5
8	120	6
9	100	5
Average	**111.1**	**5.6**

Table 5. The performance of the mobile robot equipped with gas sensors to find the odor source in mechanical turbulent airflow

No	Travel Distance (cm)	Travel Time (seconds)
1	270	18
2	260	15
3	290	25
4	260	16
5	280	23
Average	**272**	**19.4**

Table 6. The performance of the mobile robot equipped with a combination of gas sensors and wind sensors to find the odor source in mechanical turbulent airflow

No	Travel Distance (cm)	Travel Time (seconds)
1	260	13
2	260	13
3	280	14
4	280	14
5	260	13
6	260	13
7	260	13
Average	**265.7**	**13.3**

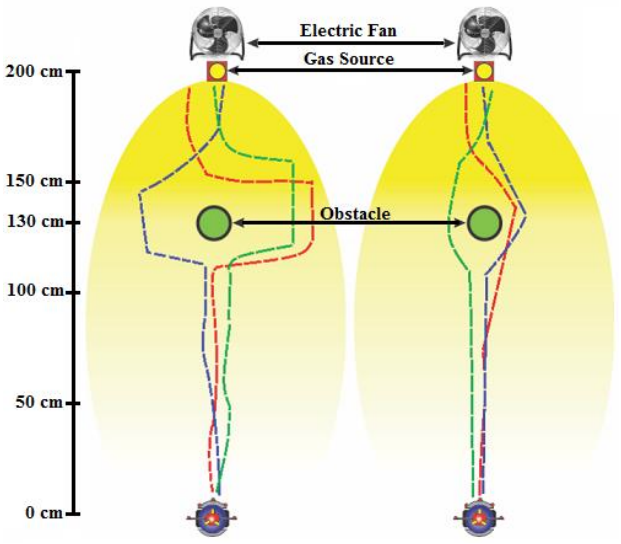

(a) (b)

Figure. 17 The robot's trajectory when tracking odor plume in mechanical turbulent airflow employing: (a) gas sensors and (b) a combination of gas sensors and wind sensors

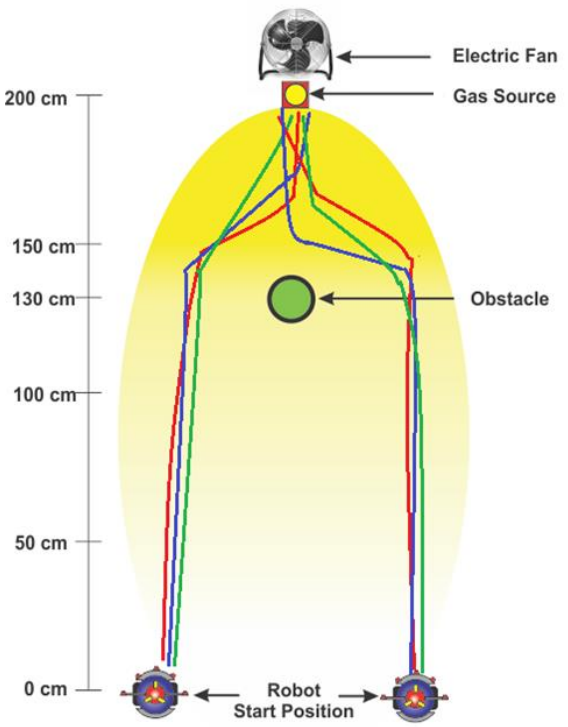

Figure. 18 The robot's trajectory when tracking odor plume in mechanical turbulent airflow employing a combination of gas sensors and wind sensors

4. Conclusion

This study has designed and realized a mobile robot equipped with gas sensors and wind sensors to find the odor source. The experimental results show that the combination of the two types of sensors can increase the success rate of 90% and 70% in laminar, and mechanical turbulent airflow, respectively, compared to the use of gas sensors only. In addition, the combination of gas sensor and wind sensor can improve the performance of the mobile robot including shorter travel distance and travel time in the search for odor source in mechanical turbulent airflow, which improve by 2.4%, and 45.9%, respectively. For future work, a robotic swarm, each equipped with gas sensors and wind sensors, is used to find odor source in outdoor environments with a high level of turbulence.

Acknowledgments

The authors would like to thank to LPPM Institut Teknologi Sepuluh Nopember (ITS) Surabaya and KEMENRISTEKDIKTI Republic of Indonesia for the financial aid support.

Reference

[1] J. Hegenberg, L. Cramar, and L. Schmidt, "Task and User Centered Design of A Human Robot System for Gas Leak Detection: From Requirements Analysis to Prototypical Realization", In: *Proc. of the 10th IFAC Symposium on Robot Control*, pp.793-798, 2012.

[2] R. Watiasih, M. Rivai, R. Wibowo, and O. Penangsang, "Path Planning Mobile Robot Using Waypoint for Gas Level Mapping", In: *Proc. of International Seminar on Intelligent Technology and Its Applications*, pp.244-249, 2017.

[3] X. Chen and J. Huang, "Odor Source Localization Algorithms on Mobile Robots: A Review And Future Outlok", *Robotics and Autonomous System*, Vol. 112, pp.123-136, 2019.

[4] B. L. Villarreal, G. Olague, and J. L. Gordillo, "Synthesis of Odor Tracking Algorithms with Genetic Programming", *Neurocomputing*, Vol. 175, Part B, pp.1019-1032, 2015.

[5] Rendyansyah, M. Rivai, and D. Purwanto, "Implementation of Fuzzy Logic Control in Robot Arm For Searching Location of Gas Leak", In: *Proc. of Intelligent Technology and Its Applications*, pp.69-74, 2015.

[6] J. Li, M. Cao, and Q. Meng, "Chemical Source Searching by Controlling a Wheeled Mobile Robot to Follow an Online Planned Route in Outdoor Field Environments", *Sensors*, Vol. 19, No. 426, pp.1-21, 2019.

[7] L. Marques, U. Nunes, and A. Almeida, "Olfaction-based mobile robot navigation", *Thin Solid Films*, Vol. 418, No. 1, pp.51-58, 2002.

[8] T. F. Lu, "Indoor Odour Source Localization Using Robot: Initial Location and Surge Distance Matter", *Robotics and Autonomous Systems*, Vol. 61, No. 6, pp.637-647, 2013.

[9] J. Li, J. Yang, S. Cui, and L. Geng, "Speed Limitation of A Mobile Robot and Methodology of Tracing Odor Plume in Airflow Environments", *Procedia Engineering*, Vol. 15, pp.1014-1045, 2011.

[10] H. Widyantara, M. Rivai, and D. Purwanto, "Wind Direction Sensor Based on Thermal Anemometer for Olfactory Mobile Robot", *Indonesian Journal of Electrical Engineering and Computer Science*, Vol. 13, No. 2, pp.475-484, 2019.

[11] A. Liberzon, K. Harrington, N. Daniel, R. Gurka, A. Harari, and G. Zilman, "Moth Inspired Navigation Algorithm in A Turbulent Odor Plume from A Pulsating Source", *PLOS ONE*, Vol. 13, No. 6, pp. 1-18, 2018.

[12] J. Monroy, V. Hernandez-Bennetts, H. Fan, A. Lilienthal, and J. Gonzalez-Jimenez, "GADEN: A 3D Gas Dispersion Simulator for Mobile Robot Olfaction in Realistic Environments", *Sensors*, Vol. 17, No. 1479, pp.1-16, 2017.

[13] F. Raynal, M. Bourgoin, C. Cottin-Bizonne, C. Ybert, and R. Volk, "Advection and Diffusion in A Chemically Induced Compressible Flow", *Journal of Fluid Mechanics*, Vol. 847, pp.228–243, 2018.

[14] W. Smyth, and J. Moum, "Three Dimensional Turbulence", *Encyclopedia of Ocean Sciences*, Vol. 6, pp.2947–2955, 2001.

[15] D. C. Eleni, T. I. Athanasios, and M. P. Dionissios, "Evaluation of the turbulence models for the simulation of the flow over a National Advisory Committee for Aeronautics (NACA) 0012 airfoil", *Journal of Mechanical Engineering Research*, Vol. 4, No. 3, pp.100-111, 2012.

[16] H. Widyantara, M. Rivai, and D. Purwanto, "Gas Source Localization Using an Olfactory Mobile Robot Equipped with Wind Direction Sensor", In: *Proc. of International Conference on Computer Engineering, Network and Intelligent Multimedia*, pp.66-70, 2018.

[17] Y. Chen, H. Cai, Z. Chen, and Q. Feng, "Using Multi Robot Active Olfaction Method to Locate Time Varying Contaminant Source in Indoor Environment", *Building and Environment*, Vol. 118, pp.101-112, 2017.

[18] P. Boeker, "Electronic Nose Methodology", *Sensor and Actuators B: Chemical*, Vol. 204, pp.2–17, 2014.

[19] S. Deshmukh, "Application of Electronic Nose for Industrial Odors and Gaseous Emissions Measurement and Monitoring – An Overview", *Talanta*, Vol. 144, pp.329–340, 2015.